Multiple responses at the boundaries of the vulnerable window in the Belousov-Zhabotinsky reaction

Rubin R. Aliev* and Alexander V. Panfilov

Department of Theoretical Biology, University of Utrecht, Padualaan 8, 3584 CH Utrecht, The Netherlands
(Received 28 November 1994)

We study vulnerability in the Belousov-Zhabotinsky reaction using experimental and numerical methods. We show that the width of the vulnerable window (VW) decreases with increasing velocity of wave propagation. A detailed study of the structure of the VW revealed a new effect: the development of multiple responses to a single premature stimulus; a single premature stimulation in a homogeneous one-dimensional medium generates two or three propagating waves. We locate this effect in the parametric space and discuss its mechanism.

PACS number(s): 05.70.Ln, 82.20.Mj

I. INTRODUCTION

The vulnerability of an excitable medium is a phenomenon that is usually connected with the dynamics of cardiac tissue after a single premature stimulation of the wake of a propagating wave; such a stimulation may result in cardiac arrhythmia [1–3]. The simplest system for studying vulnerability is a one-dimensional fiber. In a fiber an indication of cardiac arrhythmia is the occurrence of unidirectional blocking of propagation, in other words, a wave propagates in one direction but is blocked in the other. Such unidirectional blocks are usually considered to be a first step in the development of reentrant cardiac arrhythmia [1–4] (see [5] for more references).

Recently vulnerability has been observed in the Belousov-Zhabotinsky (BZ) reaction [6–9]. In addition to the fact that the study of vulnerability in a chemically active medium is itself of interest, the resemblance of wave patterns in the BZ reaction and in the heart allows one to expect the dynamics in the two systems to be qualitatively similar [9]. The results obtained in the BZ reaction can be used for an interpretation of the dynamics in the heart, where realistic experiments are laborious and difficult to carry out.

Previous theoretical studies of the vulnerability were carried out in cellular automata models [2,10] and in simple two-variable models of excitable systems [5,11,12]. It was shown that characteristic features of the phenomenon can be well understood in one-dimensional (1D) systems [10,5,13]. In 1D systems premature stimulation can cause three possible wave patterns: bidirectional, unidirectional, and decaying (blocked) propagation [5]. The region of unidirectional propagation, where in response to a local disturbance pulse propagates in one direction and is blocked in the other, is usually called the "vulnerable window" (VW) [6]. The VW corresponds to the region where vortices originate in 2D and 3D systems. Theoretical estimations [3] predict that the width of the VW is inversely proportional to the wave propagation velocity.

We have performed a detailed study of vulnerability in the BZ reaction using experimental methods and computer simulations. We study the structure of the VW and show that its width depends on the wave propagation velocity in accordance with theoretical estimations [3]. Computations with much better precision made in the vicinity of the VW boundaries revealed the following effect: the existence of a region of wave splitting, where a single premature stimulation initiates several (two or three) propagating waves. The mechanism of the phenomenon, based on the transition from unstable damped waves to stable ones, is discussed.

II. SIMULATION AND EXPERIMENTAL METHODS

Computer simulations were performed in a two-variable model of the ferroin-catalyzed BZ reaction developed by Rovinsky and Zhabotinsky [14] with rate constants estimated in Ref. [15]. The model has been verified experimentally to adequately simulate spatiotemporal phenomena in the BZ reaction [15–17]. According to the model, the dynamics in a perfectly stirred vessel is described by the differential equations for bromous acid (x) and ferriin (z) [14,15]

$$\frac{dx}{d\tau} = \frac{1}{\epsilon}\left[x(1-x) - \left(2q\alpha\frac{z}{1-z} + \beta\right)\frac{x-\mu}{x+\mu}\right] ,$$

$$\frac{dz}{d\tau} = x - \alpha\frac{z}{1-z} ,$$

where

$$[\text{Fe(phen)}_3^{3+}] = Cz , \quad [\text{HBrO}_2] = \frac{k_1 A}{2k_4}x ,$$

$$\epsilon = \frac{k_1 A}{k_4 C} , \quad \alpha = \frac{k_4 K_8 B}{(k_1 A h_0)^2} ,$$

$$\mu = \frac{k_4 k_7}{k_1 k_5} , \quad t = \frac{k_4 C}{(k_1 A)^2 h_0}\tau, \quad \beta = \frac{2k_4 k_{13} B}{(k_1 A)^2 h_0} ,$$

*Permanent address: Institute of Theoretical and Experimental Biophysics, Puschino, Moscow Region, 142292 Russia. Electronic address: rubin@wave.biol.ruu.nl

$C = [\text{Fe}(\text{phen})_3^{2+}] + [\text{Fe}(\text{phen})_3^{3+}]$,

$A = [\text{NaBrO}_3]$, $B = [\text{CH}_2(\text{COOH})_2]$,

h_0 is an acidity function, $q = 0.6$ is a stoichiometric factor, and k_i are rate constants.

The calculations were carried out for the BZ reaction of the following composition: $A = 0.25M$, $B = 0.25M$, and $C = 0.006\,25M$. To investigate the dependence of the parameters studied on the velocity of waves, h_0 was varied from 0.1 to 0.5. The composition mimics the BZ reaction recipe used for the experimental study of similar processes [6,9]. The rate constants k_i were rescaled to 18 °C using the temperature dependences described in Ref. [15]:

$k_1 = 7.9M^{-2}s^{-1}$, $k_4 = 1350M^{-1}s^{-1}$,

$k_5 = 7.94 \times 10^5 M^{-2}s^{-1}$, $k_7 = 1.19M^{-2}s^{-1}$,

$K_8 = 1.59 \times 10^{-6}M\,s^{-1}$, $k_{13} = 7.94 \times 10^{-8}s^{-1}$.

To study spatiotemporal effects, we added diffusion terms to Eqs. (1):

$$\frac{dx}{d\tau} = F(x,z) + \Delta_\rho x \ ,$$

$$\frac{dz}{d\tau} = G(x,z) + \delta\Delta_\rho z \ , \tag{2}$$

$$\rho_i = r_i \left[\frac{k_1^2 A^2 h_0}{k_4 C D_x} \right]^{0.5} .$$

Here $F(x,z)$ and $G(x,z)$ are the right-hand sides of Eqs. (1); r_i are spatial coordinates, ρ_i are scaled spatial coordinates; Δ_ρ is the Laplacian operator with respect to the coordinates ρ; $\delta = D_z/D_x$ is the ratio of the diffusion coefficients. We assume $D_x = D_z = 2 \times 10^{-5}$ cm^2 s^{-1}.

The computations were carried out in a one-dimensional array of 3000 or 12 000 elements using the Crank-Nicholson (CN) method of integration and Neumann's ("no flux") boundary conditions. The CN scheme allowed us to use a small space step, $h_x = 0.002$ mm. A time step $h_t = 0.01$ s was chosen so that the zero-dimensional system (1) could be calculated stably. To study wave splitting, the array length was increased to 12 000 elements, and the space and time steps were reduced to 0.0005 mm and 0.001 s, respectively. A further decrease in h_x and h_t did not improve the accuracy of calculations by more than a few percent, i.e., the space and time parameters measured vary by just a few percent in the finer grid.

The simulations were performed in two steps. At the beginning two or three 180 s period pulses were initiated near the left wall and passed through the medium. The next pulse was considered to be a stationary propagating reference pulse. During the second step, a stimulation was applied to the wave of a reference pulse. The simulation consisted of keeping the activator x variable on the value of 0.5 [see Eqs. (1)] for 2 s in the region of 0.2 mm width. these parameters correspond to the stimulation duration and the electrode diameter used in the experiments [6,9].

The standard technique was used for the natural experiments [6,9]: a solution of sodium bromate (0.25M), malonic acid (0.25M), ferroin (6.25 mM), and sulfuric acid was carefully stirred and poured into an 8 cm diameter Petri dish to form a layer 0.8 mm thick. After a delay of several minutes (to allow for bromomalonic acid synthesis and equilibrium) the medium was ready for the experiments. To investigate the dependence of the parameters studied on the velocity of waves, the concentration of sulfuric acid was varied from 0.1M to 0.5M.

To study the effect of vulnerability experimentally we used a protocol similar to that used in the computer simulations. First, a train of 180 s period waves was initiated somewhere near the wall of the experimental cell with a silver wire. On reaching the middle of the Petri dish, waves in such a train were regarded as planar stationary propagating reference pulses (waves were regarded as planar provided the curvature of the front was less than 0.4 cm^{-1}). Secondly, the wakes of reference pulses were stimulated with a 0.2 mm diameter silver wire by immersing the tip of the wire into the solution for 2 s. Depending on the distance from the wave front of the reference wave, the stimulation resulted in different wave patterns that were recorded on a videocassette for computer treatment with the ordinary image processing procedures as described in Refs. [6,9,18].

To compare the 2D experimental results with the 1D computer simulations we suggested that 2D circular waves initiated in the wake of a wave correspond to bidirectional propagation in 1D simulations; spiral waves correspond to unidirectional propagation; damped waves in 2D correspond to damped waves in 1D. This allowed us to plot the experimental results and computer simulations on the same figure (Fig. 2 below). A discussion of the validity of the comparison of 2D and 1D effects of vulnerability can be found in Ref. [5].

III. RESULTS

A. The vulnerable window

Typical wave patterns occurring in response to a stimulation of the wake of a wave are shown in Fig. 1. According to Ref. [5], the type of the response is determined by the site of the stimulation: stimulation in the zone of absolute refractoriness results in no waves, or in only damped propagation [Fig. 1(a)]. When stimulation is applied far behind the reference wave, i.e., to the medium at rest, it causes bidirectional propagation [Fig. 1(c)]. In the intermediate zone, unidirectional propagation is observed [Fig. 1(b)].

The width of the zone of unidirectional propagation, the VW, is shown in Fig. 2. In this figure we have plotted the data both of computer simulations and of natural experiments. The results of the natural experiments can be used to verify the validity of the use of model (1) to simulate the effect of vulnerability. The VW width measured experimentally proved to be about 1.5 times as great as that in computer simulations. There are two major reasons which explain the discrepancy: (i) we used a relatively simple two-variable model of the BZ reaction, and

(ii) the VW was measured in 2D experiments and in 1D simulations. Despite the similarity of vulnerability effects in 1D and 2D media [5], a quantitative difference should still occur. However, we regard the discrepancy of 50% as reasonable for the used class of the BZ reaction model.

Simple theoretical estimations can be made of the width of the VW [3]. That theory was originally proposed for a cellular automation model, but was then widely used to describe continuous media [5,7,8]. This is one of a few relatively simple theories which describe vulnerability effects for a wide range of parameters. The basic points of the theory are the following. Changing to a moving frame, $\xi = x - vt$, we find the VW measured in time units: t_{VW} is proportional to L/v, where L is the electrode length and v is the reference wave velocity; the VW measured in space units, l_{VW}, was assumed to be a constant [3].
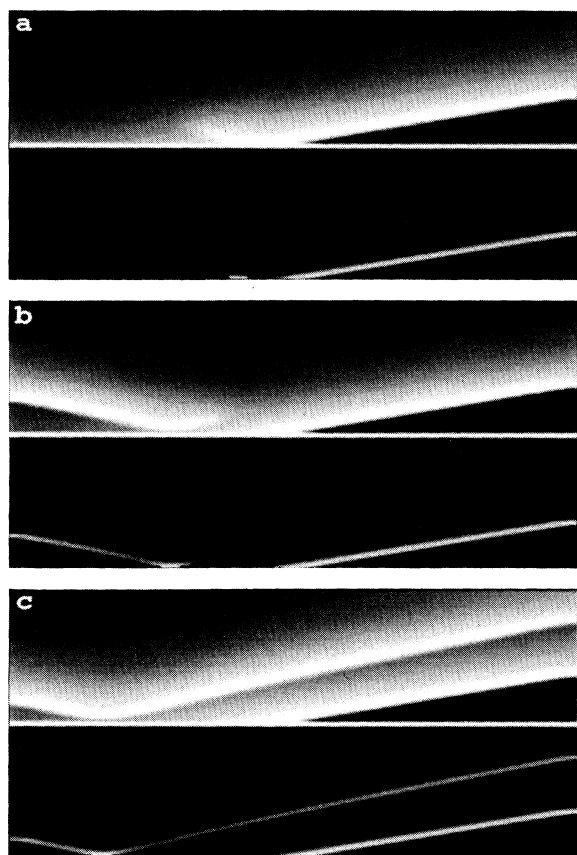

FIG. 1. Typical responses to the stimulation of the wake of a wave with a time delay Δt: (a) damping wave, $\Delta t = 16.8$ s, (b) unidirectional propagation, $\Delta t = 32.5$ s, and (c) bidirectional propagation, $\Delta t = 48$ s. Each of the sections (a)–(c) is composed of two plates presenting the spatiotemporal distribution of ferriin (upper plates) and bromous acid (lower plates). In each plate the horizontal axis stands for space in the range 0 to 6 mm; the vertical axis is time from 0 s (bottom) to 180 s (top). The reference waves are seen in the lower right-hand corners of the plates. The lighter regions correspond to the higher concentration of the species.

Our observations confirm that t_{VW} is roughly inversely proportional to v [Fig. 2(a)]. However, the line does not go through the origin. The same effect was observed in computations and is discussed in Ref. [5]. It is also seen that the experimental points do not lie exactly on a straight line. To emphasize this effect, we calculate l_{VW} which is vt_{VW}. Thus deviation from the straight line in Fig. 2(a) corresponds to deviation from the constant level of $l_{VW}(v)$ [Fig. 2(b)]. The computations show that l_{VW} is not a constant, but there is a twofold decrease of l_{VW} as v increases from 0.0018 to 0.006 cm/s. Despite the large scatter of the experimental points [Fig. 2(b), circles], one can see a similar change in the experimentally measured l_{VW}. The origin of the experimental errors is discussed below.

The physical meaning for the nonstationarity of l_{VW} [Fig. 2(b)] and the deviation of t_{VW} from a straight line [Fig. 2(a)] is a deformation of the pulse shape with changing propagation velocity. This, in turn, results in a change in the refractory tail and the VW.

The boundaries of the VW are shown in Fig. 3. The curves in this figure divide the plane into regions where different wave patterns occur. Below the curves depicting the left VW boundary there is no stable propagation,
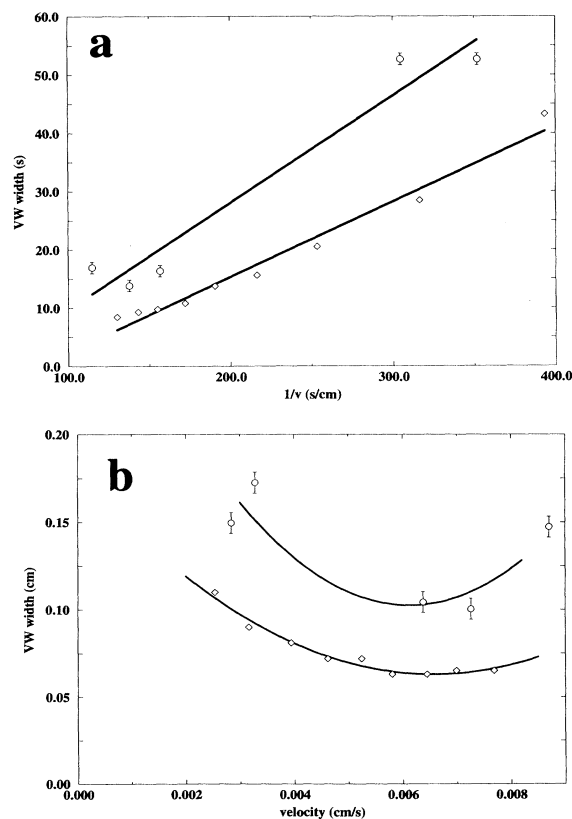

FIG. 2. Vulnerable window width vs reference wave velocity. The VW measured in time units (a) is invesely proportional to velocity, as predicted by the theory [3]. In contrast, the VW measured in space units (b) is not a constant. Circles represent experimental data and diamonds computer simulations.

but damped pulses occur. This curve fences in a region conventionally called the region of "absolute refractoriness." Above the curve of the right VW boundary, bidirectional propagation occurs. In this region the medium is at rest. Between the two regions unidirectional propagation (VW) is observed.

B. Splitting the waves

The above-mentioned conventional classification of wave patterns adequately describes the dynamics of a system far away from the boundaries of the VW. Near the boundaries damped propagating pulses appear; these are usually regarded as decaying pulses [19,20,5]. We studied the dynamics of such damped pulses and found that the decay is not the only way of their evolution. Under the appropriate conditions damped pulses can transform into stably propagating pulses which qualitatively change the wave patterns in the system.

As a stimulation is applied near the boundary of the VW (near the curves in Fig. 3), multiple responses occur after only one stimulation. Figure 4 shows wave patterns that have arisen after a stimulation near the left boundary of the VW. Double responses on plates (b) and (c) are seen between the regions of damped (a) and unidirectional (d) propagation. A similar effect is shown in Fig. 5, where triple responses (b) and (c) occur near the right VW boundary. The wave patterns depicted can be interpreted as a wave splitting.

To understand the phenomenon one should note that after initiation a pulse moves in the wake of a reference wave, i.e., it moves with gradually decreasing amplitude (Fig. 6) and velocity (Fig. 7). The difference in propagation velocities results in an increase in the distance between the reference wave and the pulse. Such a damped pulse would die out (Fig. 6, circles), unless it crossed the boundary of the region of absolute refractoriness with a large enough amplitude to initiate a new stably propagating wave (Fig. 6, diamonds).

The dynamics of the change of a damped pulse to a stationary propagating one can be divided into several distinct stages. During the first stage ($t = 0$–30 s) there is a decrease in the amplitude and velocity of the pulse, until
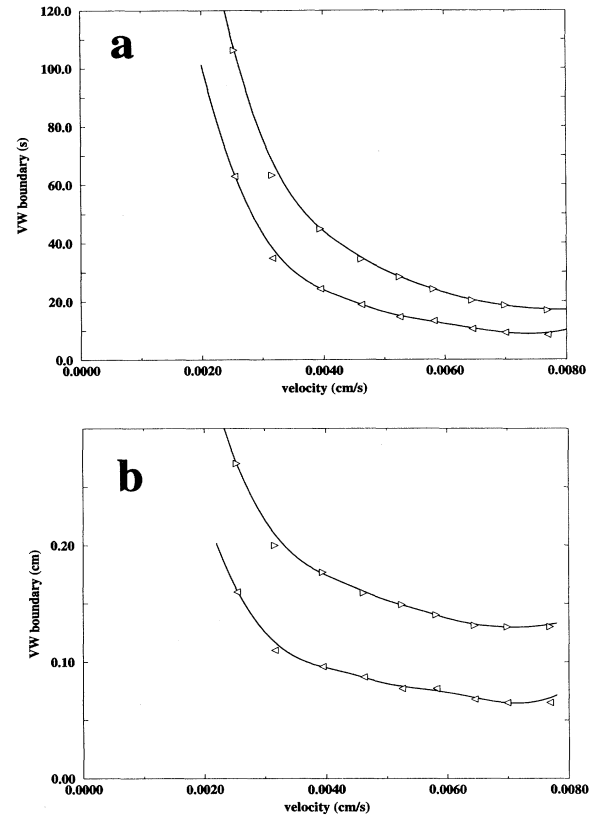

FIG. 3. Left boundary (upward triangles) and right boundary (downward triangles) of the VW measure din (a) time units and (b) space units as functions of the reference wave velocity.

the pulse almost stops (Figs. 6 and 7). Then ($t = 30$–42 s) the pulse increases in amplitude (Fig. 6, diamonds), but still moves with low velocity (Fig. 7). During the third stage ($t = 42$–45 s) the pulse intersects the boundary of absolute refractoriness and quickly starts to gain velocity (Fig. 7), forming a stably propagating wave ($t = 45$–65 s).

Figure 8 shows a plot of the number of responses vs the time delay. This plot has a hierarchical structure. There are three wide regions: (i) of zero responses
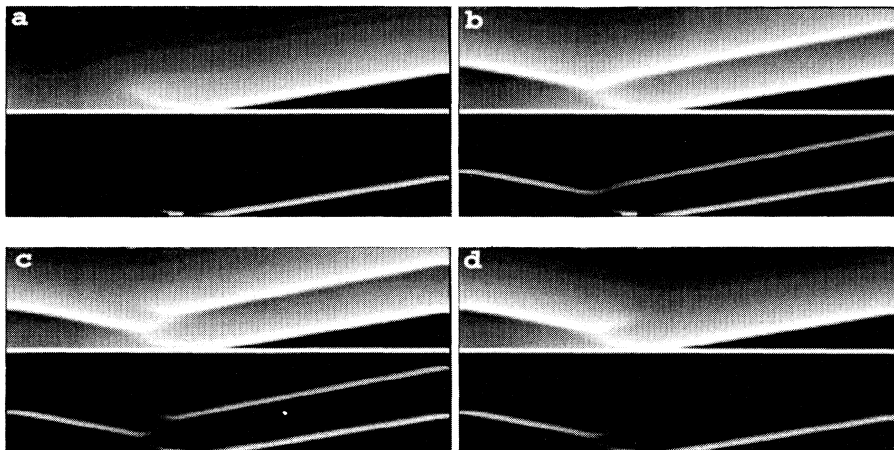

FIG. 4. Multiple responses near the left boundary of the VW. (a) Damped propagation, $\Delta t = 17.55$ s; (b) and (c) double response, $\Delta t = 17.58$ and 17.71 s; (d) unidirectional propagation, $\Delta t = 17.73$ s. Note the split damped waves in (c) and (d).
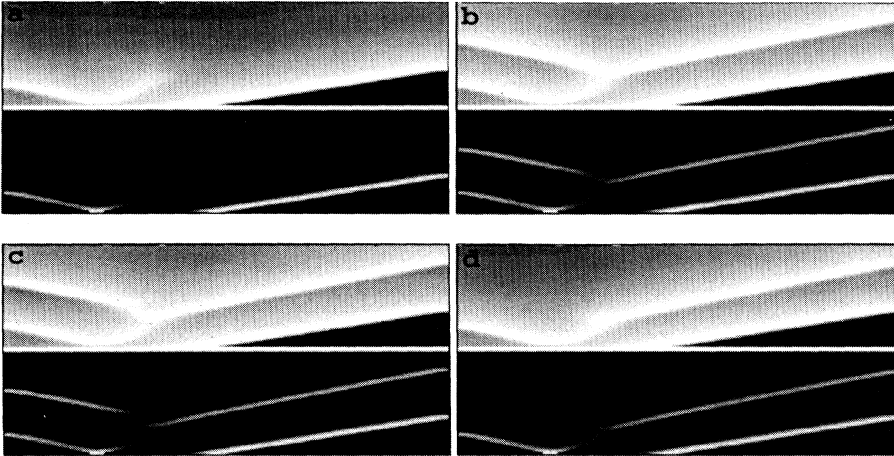
FIG. 5. Multiple responses near the right boundary of the VW. (a) Unidirectional propagation, $\Delta t = 37.60$ s; (b) and (c) triple response, $\Delta t = 37.61$ and 37.63 s; (d) double response, $\Delta t = 37.74$ s. Note that the fourth split (although decayed) response is seen in (c).

($\Delta t = 0–17.55$ s), (ii) of one response ($\Delta t = 17.73–37.60$ s), and (iii) of two responses ($\Delta t > 37.64$ s). These regions correspond to the conventional classification of responses as "damped," "unidirectional" (VW), and "bidirectional" propagation [5]. Near the boundaries between these regions, small areas of unusual double and triple responses occur. Such multiple responses are caused by the wave splitting described above.

Obviously, using the transformation $\Delta l = v \Delta t$, one can plot a graph of the number of responses vs the spatial delay Δl (the distance between a premature stimulation and a reference wave) which has a structure similar to that shown in Fig. 8.

IV. DISCUSSION

The wave splitting described above bears some resemblance to the dynamics described by Yakhno and co-workers in the FHN model with special symmetry requirements [21–23]. They found that under appropriate conditions a propagating front stops and starts splitting; this is seen as a wave source. The effect was called the "stopped front division" [21–23]. These papers reported

the occurrence of an infinite wave train.

The width of the window where wave splitting occurs is narrow [Fig. 8]. This is why we did not observe the effect in our experiments. The experimental points presented in Fig. 2 illustrate the dependence of the VW on the wave velocity. It should be noted that the experi-

FIG. 7. Propagation of a damped wave (diamonds, $\Delta t = 7.58$ s) in the wave of a reference wave (circles). (a) Wave crest position and (b) velocity. Jumps on the position and velocity curves correspond to transitions to a stably propagating pulse. The curve through the diamonds was plotted after the median filtration of the data.
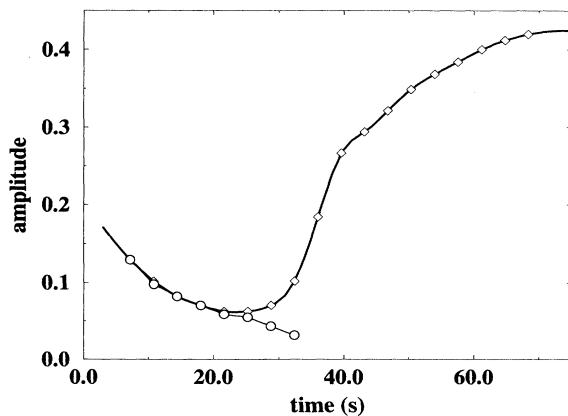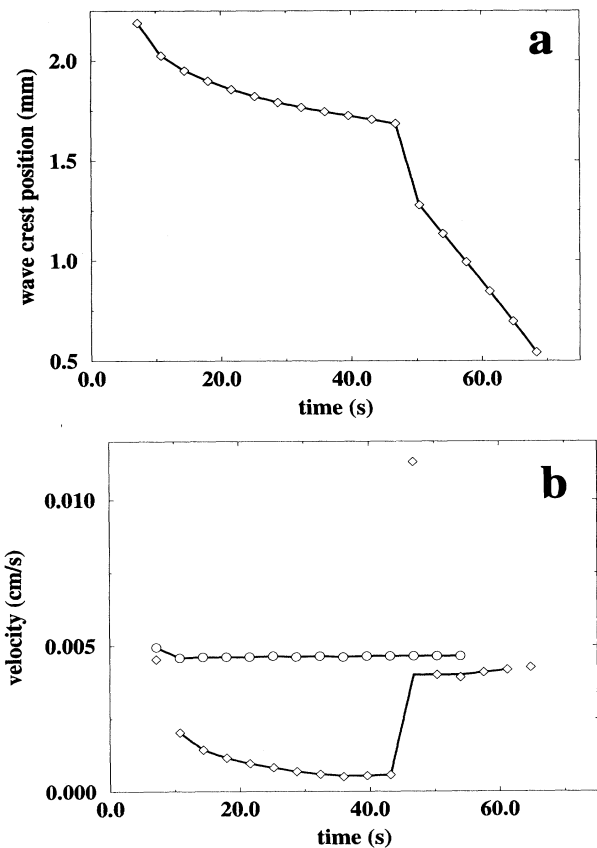

FIG. 6. Amplitude of damped waves [x variable in Eqs. (1)] in the wake of a reference wave. Two kinds of dynamics are possible for damped waves: decay (circles, $\Delta t = 17.55$ s) or transition to a stably propagating pulse (diamonds, $\Delta t = 17.58$ s).
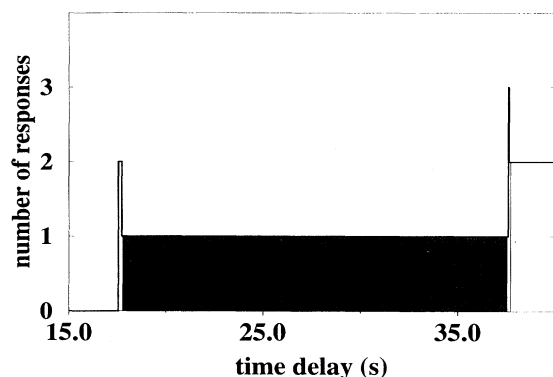
FIG. 8. The number of responses vs time delay of the stimulation. The shaded area between 17.73 and 37.60 s corresponds to the VW. Multiple responses near the VW boundaries occur due to wave splitting.

mental points in Fig. 2(a) are divided into two clusters. We used linear regression to fit the points for the following reasons: (i) the linear dependence of the VW on $1/v$ is predicted by the theory [3], and (ii) the linear dependence is evident in computer simulations.

Comparison of the results of experiments and simulations shows that there is large scatter in the experimentally measured points. The error bars in Fig. 2 correspond to the roughness of measuring space and time units while using a computerized image processing system, e.g., the precision of the space measurements is restricted to one pixel of a 512×512 pixel frame. In addition to such device dependent errors there are processes occurring inevitably in the system resulting in significant scattering of experimental data. These are the deformation of the surface of the solution while immersing the reference electrode, some hydrodynamic flow arising in the system, and deformations of the shape of the reference pulse. These disturbing effects are difficult to take into account. Experimental difficulties do not allow us to obtain enough probes to use statistical methods to evaluate the errors. One possible solution is the use of computer simulations to study the effects. The computer results have small scatter of the data and are rather close to the experimentally observed results. Thus we cannot avoid large scattering of experimental data, but can use computational results to predict the dynamics in the system.

Another experimental technique was used in Refs. [7,8]. The researchers observed a narrow band of bidirectional propagation (circular waves) between the regions of decaying and unidirectional propagation (spiral waves). The authors gave a different explanation for the effect, but we believe the effects described in Refs. [7,8] can be understand in terms of wave splitting. However, a much better experimental technique is required if wave splitting in the BZ reaction is to be investigated experimentally.

In this paper we compare the results of 2D experiments and 1D numerical simulations. To make this reasonable, we used planar 2D waves in the experiments as reference waves. We referred to the resemblance of 2D and 1D vulnerability effects (e.g., see Ref. [5]). Actually, the 2D and 1D effects are not the same, but have some quantitative discrepancies (Fig. 2).

Recent computational studies of similar problems [6–8] have failed to discover wave splitting because in these papers damped waves were always regarded as decaying waves. As a rule, Euller's explicit scheme of integration was used to study the dynamics, which imposed substantial restrictions on space and time steps. Small space steps are essential to observe the wave splitting.

It is possible to evaluate the critical value of the space step. Actually, the shortest time and space scales are connected with the increase of $HBrO_2$ smeared by a Laplacian. According to the FKN scheme of the BZ reaction [24] this is an exponential process. This process is accounted for in Eq. (1). Actually, the growth of $HBrO_2$ can be described as $dx/d\tau = x/\epsilon$ [see Eq. (1)] with the characteristic time $t_{char} = \epsilon$. Expressed in seconds, the shortest time scale $t_{char} = 2$ s. The space scale can be evaluated as $l_{char} = v t_{char}$. For ordinary propagating waves $l_{char} = 0.01$ cm. To observe wave splitting, we should simulate waves whose velocity v is ten times lower [Fig. 7(b)]. This results in the ten times finer grid required. The space step h_x is usually chosen to place 5 to 20 lattice points on l_{char}. The value of h_x thus evaluated should be lower than 0.0002 cm.

The mechanism of the wave splitting which is based on the transition of damped pulses to stationary propagated ones seems to be of a general nature and is likely to occur in other excitable systems. The window where the wave splitting occurs is narrow in the BZ reaction medium used, but it can be wider in other excitable media, e.g., in heart tissue, where the study of vulnerability is of practical importance.

ACKNOWLEDGMENT

[1] G. R. Mines, Trans. R. Soc. 4, 45 (1914).

[2] N. Wiener and A. Rosenblueth, Arch. Inst. Cardiol. Mex. 16, 205 (1946).

[3] V. I. Krinsky, Biofizika 11, 676 (1966).

[4] J. P. Keener, Math. Biosci. 90, 3 (1988).

[5] C. F. Starmer et al., Biophys. J. 65, 1775 (1993).

[6] C. F. Starmer et al., in Spatio-Temporal Organization in Nonequilibrium Systems, edited by S. C. Muller and T. Plesser (Project Verlag, Dortmund, 1992).

[7] M. Gómez-Gesteira et al., Physica D 76, 359 (1994).

[8] G. Fernández-García et al., Eur. J. Phys. 15, 221 (1994).

[9] R. R. Aliev, Chaos, Solitons and Fractals 5, 567 (1995).

[10] A. Rosenblueth, J. Alanis, and J. Mandoki, J. Cell. Comp. Physiol. 33, 405 (1949).

[11] B. Y. Kogan *et al.*, Physica D **50**, 327 (1991).

[12] J. Starobin, Y. I. Zilberter, and C. F. Starmer, Physica D **70**, 321 (1994).

[13] W. Quan and Y. Rudy, Circ. Res. **66**, 367 (1990).

[14] A. B. Rovinsky and A. M. Zhabotinsky, J. Phys. Chem. **88**, 6081 (1984).

[15] R. R. Aliev and A. B. Rovinsky, J. Phys. Chem. **96**, 732 (1992).

[16] R. R. Aliev and K. I. Agladze, Phyica D **50**, 65 (1991).

[17] R. R. Aliev and V. N. Biktashev, J. Phys. Chem. **98**, 9676 (1994).

[18] R. R. Aliev, J. Phys. Chem. **98**, 3999 (1994).

[19] K. Maginu, J. Math. Biol. **6**, 49 (1978).

[20] K. Maginu, J. Math. Biol. **10**, 133 (1980).

[21] V. G. Yakhno, Biofizika **20**, 669 (1975).

[22] G. M. Zhislin, V. G. Yakhno, and Y. K. Gol'tsova, Biofizika **21**, 693 (1976).

[23] V. G. Yakhno, Y. K. Gol'tsova, and G. M. Zhislin, Biofizika **21**, 1067 (1976).

[24] R. J. Field, in *Oscillations and Traveling Waves in Chemical Systems*, edited by R. J. Field and M. Burgers (Wiley, New York, 1985), pp. 55–92.
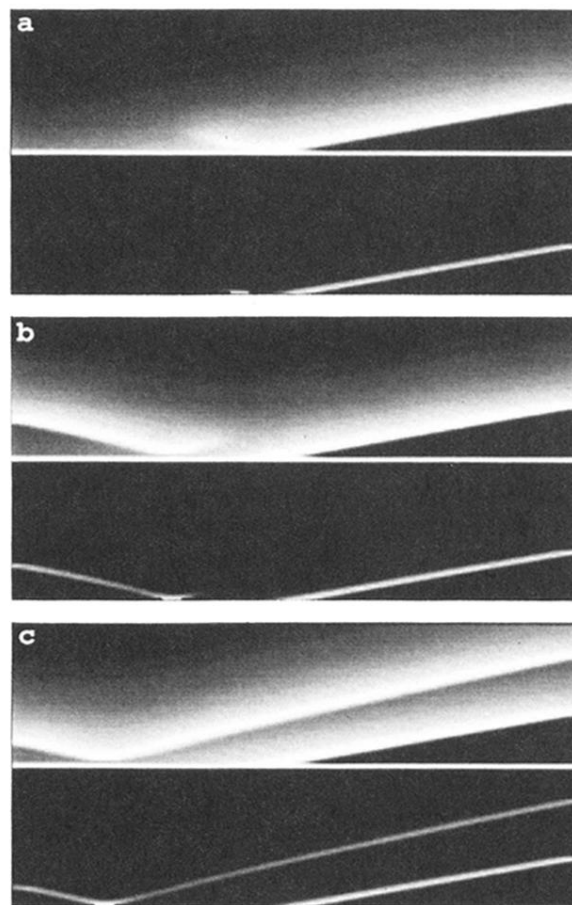
FIG. 1. Typical responses to the stimulation of the wake of a wave with a time delay Δt: (a) damping wave, $\Delta t = 16.8$ s, (b) unidirectional propagation, $\Delta t = 32.5$ s, and (c) bidirectional propagation, $\Delta t = 48$ s. Each of the sections (a)–(c) is composed of two plates presenting the spatiotemporal distribution of ferri-in (upper plates) and bromous acid (lower plates). In each plate the horizontal axis stands for space in the range 0 to 6 mm; the vertical axis is time from 0 s (bottom) to 180 s (top). The reference waves are seen in the lower right-hand corners of the plates. The lighter regions correspond to the higher concentration of the species.
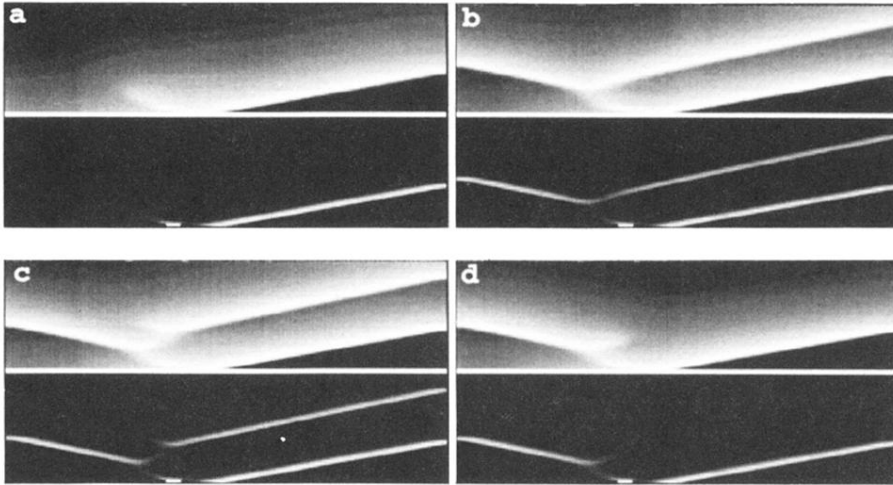
FIG. 4. Multiple responses near the left boundary of the VW. (a) Damped propagation, $\Delta t = 17.55$ s; (b) and (c) double response, $\Delta t = 17.58$ and 17.71 s; (d) unidirectional propagation, $\Delta t = 17.73$ s. Note the split damped waves in (c) and (d).
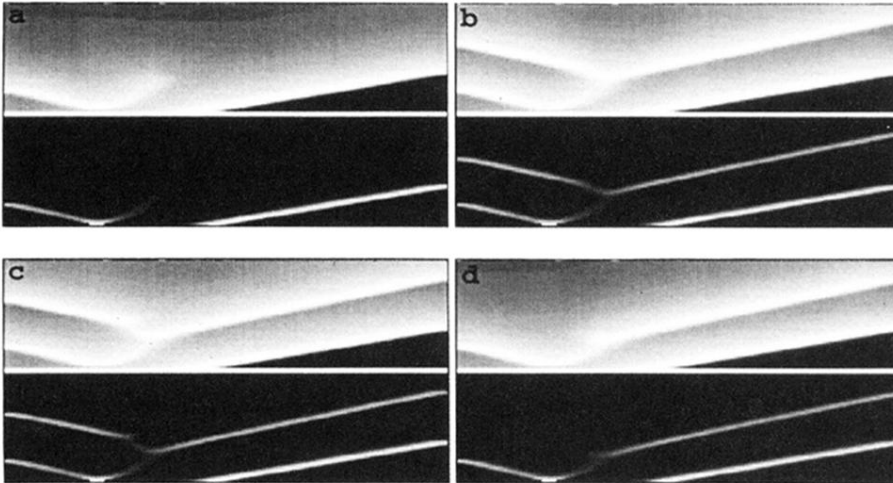
FIG. 5. Multiple responses near the right boundary of the VW. (a) Unidirectional propagation, $\Delta t = 37.60$ s; (b) and (c) triple response, $\Delta t = 37.61$ and 37.63 s; (d) double response, $\Delta t = 37.74$ s. Note that the fourth split (although decayed) response is seen in (c).
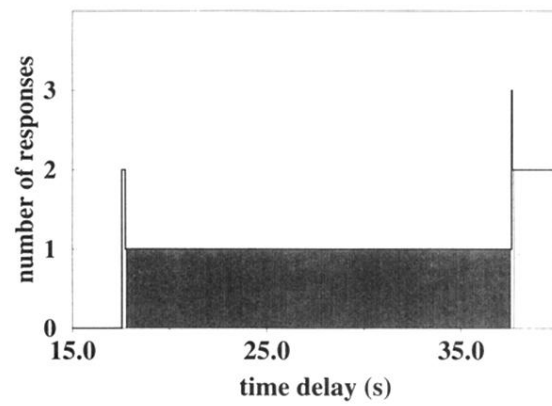
FIG. 8. The number of responses vs time delay of the stimulation. The shaded area between 17.73 and 37.60 s corresponds to the VW. Multiple responses near the VW boundaries occur due to wave splitting.